THE EFFECTS OF ATMOSPHERIC AND OCEANIC CONDITIONS ON THE STABILITY OF ICE BRIDGES

by

Sigourney Anne Stelma

A thesis submitted to the Faculty of the University of Delaware in partial fulfillment of the requirements for the degree of Master of Science in Marine Studies

Spring 2015

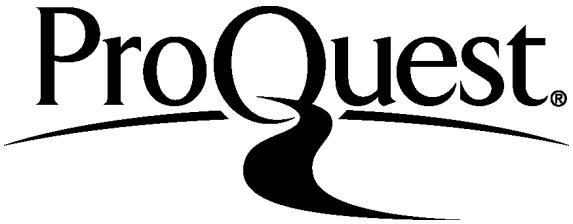

THE EFFECTS OF ATMOSPHERIC AND OCEANIC CONDITIONS ON THE STABILITY OF ICE BRIDGES

by

Sigourney Anne Stelma

Approved: _____

Helga Huntley, Ph.D.
Professor in charge of thesis on behalf of the Advisory Committee

Approved: _____

Mark Moline, Ph.D.
Director of the School of Marine Science and Policy

Approved: _____

Nancy Targett, Ph.D.
Dean of the College of Earth, Ocean and Environment

Approved: _____

James G. Richards, Ph.D.
Vice Provost for Graduate and Professional Education

ACKNOWLEDGMENTS

Advisor: Dr. Helga Huntley

CICE creator: Dr. Elizabeth Hunke

Committee members: Dr. Andreas Muenchow and Dr. Sara Rauscher

PhD Student: Patricia Ryan

Robinson 210

TABLE OF CONTENTS

LIST OF TABLES

LIST OF FIGURES

ABSTRACT

Ice bridges are arch-like ice structures that form in narrow passages and straits. These bridges play largely important roles in the circulation of Arctic sea ice. When an ice bridge is present in a strait, there is typically a stoppage of sea ice flow, and there generally little ice flow downstream from the bridge. Nares Strait, located between Ellesmere Island and Greenland, allows for Arctic sea ice to be exported into the Atlantic Ocean. Ice bridges typically form in Nares Strait, which causes a stoppage of this export. This stoppage allows for Arctic sea ice to grow thicker, which is important for our current climate. Building on studies that examined the formation of ice bridges, this study aims to model and analyze the destruction of ice bridges.

Using CICE: The Los Alamos Sea Ice Model, ice bridges are modeled in an idealized strait that is geographically and dimensionally similar to Nares Strait. The bridges are allowed to strengthen for 7 days past their initial formation. Then various atmospheric and oceanic parameters are changed, to examine their effect on the stable ice bridges. All parameter changes are applied over the entire domain and are constant in time.

Extreme temperatures are used to study the effect of temperature. Then various amounts of longwave and shortwave radiation are tested independently, combined with temperature and combined with each other and temperature. We found that air temperature alone isn't the driving mechanism in bridge disintegration. As for radiative forcing, longwave radiation proves to have a stronger effect than shortwave radiation. In fact, when air temperature, longwave radiation and shortwave radiation are combined, longwave radiation is the most dominant factor in disintegrating the bridges, followed by air temperature. Wind

and currents are also tested. A seasonal progression, from winter to summer, is also applied to stable ice bridges of different initial thicknesses. All bridges studied under the seasonal progression were destroyed within the three season time constraint.

Chapter 1

INTRODUCTION

The Arctic Ocean has several passageways connecting it to the other oceans, as seen in Figure 1.1. The Bering Strait, located in between the United States and Russia, accounts for the majority of flow into the Arctic Ocean (Woodgate & Aagaard, 2005). The flow through the many narrow straits located in the Canadian Arctic Archipelago is almost entirely southward. Finally, there are several large passageways in the Nordic Seas, the largest being Fram Strait, which allow both in- and outflow. The dynamics of exchanges of both water and ice between the Arctic and other oceans is a crucial piece of the global circulation system. Its exchanges, of course, also have a large impact on the Arctic Ocean itself, possibly more so than for most other ocean basins, due to its unique role as reservoir of freshwater in the form of ice.

The extent of multiyear sea ice in the Arctic Ocean has been decreasing since the early 1980's (Parkinson & Cavalieri, 2008). Ice export is a significant factor in the depletion of Arctic sea ice. There are several passageways that allow for flow into and out of the Arctic. Kwok (2009) calculated annual and seasonal area ice flux means for Fram Strait and two passageways leading into the Barents Sea from radiometer data. Fram Strait's ice gate is 410km wide, while the other two locations, between Svalbard and Franz Josef Land (S-FJL) and between Franz Josef Land and Severnaya Zemlya (FJL-SZ), have 295km and 417km ice gates, respectively. The annual mean ice flux through Fram Strait over a 29-year period was 706 x 10^3km^2 with a summer mean of 91 x 10^3km^2. S-FJL had an annual mean ice flux of 37 x 10^3km^2 while FJL-SZ actually had a mean inflow of 103 x 10^3km^2 (Kwok, 2009). Kwok *et al.* (2004) calculated the mean annual ice volume flux through Fram Strait to be about

Figure 1.1: The Arctic Region. Adapted from The University of Texas at Austin

2200km^3/yr. Since the annual ice flux out of Fram Strait is so large, significantly larger than the ice flux out of S-FJL, Fram Strait is a key passageway for sea ice flux out of the Arctic. However, other Arctic passageways are also important.

The significantly smaller straits in the Canadian Arctic Archipelago account for a much smaller fraction of the ice export. Yet they play the role of gate-keeper: Due to

their geometry, ice blockages frequently arise, keeping the ice in the Arctic and permitting the growth of multiyear ice. Most of the passages through the Archipelago are clogged with ice for much of the year, making the infamous Northwest Passage so challenging to navigate (Melling, 2002). Nares Strait, the body of water separating Greenland from the Canadian Ellesmere Island (Figure 1.2), provides a direct link between the Arctic Ocean and the Atlantic Ocean. Due to the circulation patterns in the Arctic, it constitutes the preferred pathway for ice export through the Canadian Arctic Archipelago (Melling, 2000).

Nares Strait, with an ice gate of only 30km, had a mean annual ice area flux of 33 x 10^3km^2 over 1996-2002, less than 1/20 of that through Fram Strait but comparable to that through the much wider S-FJL (Kwok, 2005). The ice passing through Nares Strait tends to be thicker: The average thickness of the Arctic ice north of Nares Strait is around 4-5m, significantly thicker than the basin-wide winter average thickness of about 2.9m (Kwok *et al.* , 2010). Thus, ice flow through Nares Strait contributes disproportionately to the multiyear ice export.

Ice flux through Nares Strait is also more variable than that through Fram Strait. For example, in 2007 the mean ice area flux was 87 x 10^3km^2 (Kwok *et al.* , 2010), more than 2.5 times the 13-year mean. The ice volume flux that year also exceeded twice its 13-year mean. While the ice outflow through Fram Strait was also anomalously high in the summer of 2007, the volume exported at Nares Strait was more than 10% of the mean ice export at Fram Strait.

Clearly, 2007 was an anomalous year for ice flux through Nares Strait. That year was also unusual in that no ice bridge formed in the strait (Kwok *et al.* , 2010). Ice bridges are arch-like ice blockages that form in narrow passages and straits. As illustrated by events in 2007, these bridges critically affect Arctic sea ice export. When an ice bridge is present, even the ice downstream from the bridge tends to flow more slowly (Hibler *et al.* , 2006).

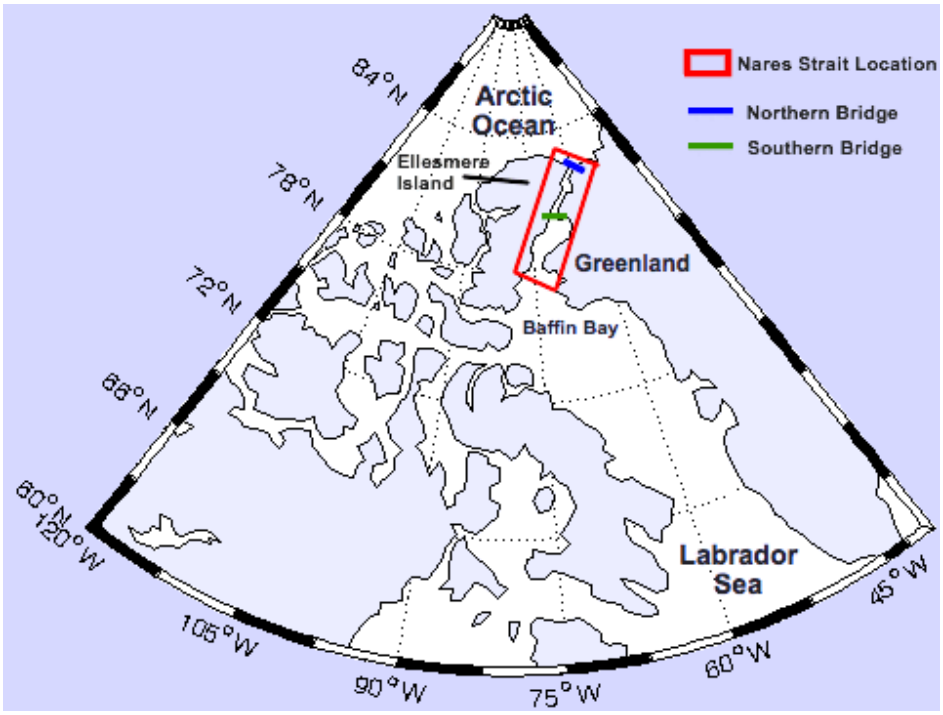

Figure 1.2: Nares Strait (highlighted in red) and surrounding bodies of water. The approximate locations of ice bridges that typically form in the strait are indicated in blue and green.

In Nares Strait, bridges typically form at two locations (Figure 1.2). Bridge formation at the entrance to Robeson Channel is known as the northern bridge, while the southern bridge location is at Kane Basin. Both types of bridges typically last for 5-7 months (Kwok *et al.* , 2010). Once these bridges are formed, they are able to withstand winter and spring atmospheric and oceanic conditions.

1.1 Implications of No Bridge Formation

When the Nares Strait bridges do not form, significant amounts of multiyear ice leave the Arctic (Kwok *et al.* , 2010). Decreasing multiyear ice in the Arctic will have dramatic effects on climate. A decrease in multiyear ice will allow for the ice to melt faster and bridges will be less likely to form, thus causing a decrease in sea ice extent. Decreasing

sea ice extent will increase heat, momentum and water vapor exchange between the ocean and the atmosphere. Vihma (2014) and studies cited therein, have shown that with an increase of heat flux into the ocean, air temperatures in the Arctic have increased in autumn and early winter. These studies also show that there has been a local increase in evaporation, air moisture, cloud cover and precipitation. Another implication is that the surface albedo will decrease with a decrease in sea ice extent. This albedo reduction will cause increased heating of the ocean in summer. Higher ocean temperatures will cause a delayed freezing season for Arctic sea ice. These implications, in turn, will contribute to further sea ice decline.

Bridge formation also has an effect downstream. When no ice bridges formed in Nares Strait in 2007, the ice area and volume fluxes through the strait were more than twice their 13-year mean (Kwok *et al.* , 2010). An increased output of sea ice from Nares Strait to the Labrador Sea and Atlantic Ocean can impact salinity in these areas. Cheng & Rhines (2004) conducted a modeling study to observe the implications of increased positive freshwater flux from the Arctic on the Meridonal Overturning Circulation (MOC). They determined that Labrador Sea water plays a more significant role in the MOC than overflows across the Greenland-Scotland Ridge. They found that adding 0.1 Sv ($10^6 m^3/s$) of freshwater to the Nordic Seas reduces the overturning in the Atlantic Ocean by 1-2 Sv. When 0.1 Sv of freshwater flux was added to the southern Baffin Bay area, the MOC was reduced by 3-5 Sv.

Ice bridge formation is essential for the formation of the North Water (NOW) polynya. A polynya is an area of open water surrounded by ice. This polynya typically forms during the winter-spring period in northern Baffin Bay and is the largest in the Arctic (Dumont *et al.* , 2010). The strong northerly winds prevalent in Nares Strait move ice downstream from a formed ice bridge. This leaves behind an open area of water, or polynya. Studies have shown that this polynya supports marine mammals and birds (Stirling, 1997). Primary production in the NOW polynya is among the highest in the Arctic. This is partially

due to an early bloom in areas of shallow mixed layers (Tremblay *et al.* , 2002), which result from storms over the polynya. Tremblay *et al.* (2002) also suggested that the storm winds entrain nutrients from deeper waters to the surface. In addition, they found evidence that the primary production in the NOW polynya will respond to atmospheric and oceanic changes associated with climate change. Dumont *et al.* (2010) suggest that strong winds likely produce strong upwelling events along Greenland's coast, which are extended by the presence of an ice bridge.

In summary, as the ice thins due to warming in the Arctic, stable ice bridge formation becomes less likely (see also Chapter 3). The positive feedback cycle leading to greater warming and even thinner ice will exacerbate this effect. Without an ice bridge, the NOW polynya cannot form and support the wildlife dependent on its primary production. Lastly, farther reaching consequences of this local event in Nares Strait are tied to the salinity anomalies in the Labrador Sea due to ice export, which have been shown to affect the MOC.

1.2 Bridge Formation and Disintegration

Clearly, whether an ice bridge forms in a given year and when, has significant impacts on both the local and the regional oceanic and atmospheric conditions. Modeling studies have been used to determine what atmospheric and oceanic parameters are essential for bridge formation (Dumont *et al.* , 2009; Kubat & Sayed, 2006). Of similar importance is the disintegration of ice bridges, as short lived bridges are less effective for growing multi-year ice, reducing its export and supporting a polynya. The question then arises what kind of atmospheric and oceanic conditions promote bridge destruction?

Dumont *et al.* (2009) modeled the formation of ice bridges in an idealized strait. They used the Geophysical Fluid Dynamics Laboratory (GFDL) ice model, based on the elastic-viscous-plastic (EVP) rheology of Hunke & Dukowicz (1997), which is coupled to the Modular Ocean Model (MOM). For simplicity, they neglected the effects of thermodynamics as well as the Coriolis force. Their domain was designed to mimic the geography around

the NOW polynya. They included a wide basin that converges into a narrow channel, which then opens up again. An ice pack of 100% concentration was initialized in the top half of the domain, ending at the first constriction point. To represent the strong winds present in Nares Strait, a constant northerly wind stress value of 0.20Nm^{-2} was applied. Closed boundary conditions were used for the simulations. A sensitivity study was conducted, varying initial thickness h_0 and the shear strength parameter e (See Section 2.2 for more details on e.)

The present study seeks to extend the work of Dumont *et al.* (2009) by focusing on the end of the life of ice bridges. We have chosen CICE: The Los Alamos Sea Ice Model in its uncoupled implementation, along with an idealized domain similarly designed to mimic conditions in Nares Strait. In order to better relate the two studies, we repeated the analysis of bridge formation criteria with our model and domain, as well as applying it to more realistic conditions such as accounting for thermodynamics and the Coriolis force, opening the boundaries and using a much smaller computational time step. (See Section 2.4 for a discussion of the choice of time step and model convergence.)

As discussed in greater detail in Section 3, our findings are broadly consistent with those of Dumont *et al.* (2009), but the more realistic analysis shifts the bridge formation region in parameter space.

The main aim of this project, however, is to examine how changes in atmospheric and oceanic parameters affect the stability of ice bridges. The main parameters varied are air temperature, radiative forcing, wind and currents. Air temperature was chosen and tested first because it is the most intuitive parameter. As temperature increases, ice thickness decreases due to the added heat. Radiative forcing was tested next, as it also will introduce added heat flux into the system. Wind and currents were chosen as they are two important dynamic parameters.

Chapter 2 describes the model and previews where the aforementioned parameters fit into the model. Chapter 3 describes the formation of ice bridges using CICE. The results

and discussion are provided in Chapter 4. Finally, this document is concluded in Chapter 5 with a summary of the findings and related conclusions.

Chapter 2

METHODS

2.1 Model

CICE has several interactive components, including a model of ice dynamics and a model of thermodynamics. The fundamental equations solved by CICE describe the evolution of ice thickness distribution in time and space and momentum conservation, namely:

$$\frac{\partial \gamma}{\partial t} = -\nabla \cdot (\gamma \boldsymbol{u}) - \frac{\partial}{\partial h}(f_t \gamma) + \psi, \tag{2.1}$$

where γ is the ice thickness distribution function, $\nabla = \left(\frac{\partial}{\partial x}, \frac{\partial}{\partial y}\right)$, $\boldsymbol{u}$ is the horizontal ice velocity, f_t is the rate of thermodynamic growth and ψ is the ridging redistribution function,

and

$$m\frac{\partial \boldsymbol{u}}{\partial t} = \nabla \cdot \sigma + \vec{\tau}_a + \vec{\tau}_w - \hat{k} \times mf\boldsymbol{u} - mg\nabla H_o, \tag{2.2}$$

where m is mass per unit area, σ is ice stress, $\overrightarrow{\tau_a}$ is wind stress, $\overrightarrow{\tau_w}$ is ocean stress, f is the Coriolis parameter, g is acceleration due to gravity and H_o is sea surface height.

The three terms on the right-hand side of (2.1) describe advection, transport in thickness space (h) due to thermodynamic growth and melting, and transport in thickness space (h) due to ridging and mechanical processes, respectively. The last two terms on the right-hand side of (2.2) describe stress due to Coriolis effects and the sea surface slope, respectively.

The equations are discretized using a remapping scheme and a generalized orthogonal B-grid.

2.2 Elastic-Viscous-Plastic Model

A rheology describes the deformation and flow of matter. This is important for modeling the dynamics of sea ice. The viscous-plastic (VP) rheology introduced by Hibler (1979) became the first widely used sea ice dynamics formulation. Hunke & Dukowicz (1997) modified the VP model by adding an elastic term, primarily to account for undesirable numeric effects, and created what is known as the elastic-viscous-plastic (EVP) model, which is used by CICE.

The viscous-plastic (VP) rheology is given by a constitutive law relating internal ice stress σ_{ij} and the rates of strain $\dot{\epsilon}_{ij}$. This is done through the use of an internal ice pressure P, nonlinear bulk viscosity ζ and shear viscosity η. The principal components of stress lie on an elliptical yield curve, where the ratio of major to minor axes is e. Hibler (1979) originally used $e = 2$. This rheology allows for divergence of the ice pack but resists shearing and the compression associated with convergence. The larger the value of e, the less cohesive the ice is. The constitutive law is:

$$\dot{\epsilon}_{ij} = \frac{1}{2\eta}\sigma_{ij} + \frac{\eta - \zeta}{4\eta\zeta}\sigma_{kk}\delta_{ij} + \frac{P}{4\zeta}\delta_{ij} \tag{2.3}$$

The ellipse parameter e appears in the expressions for the bulk and shear viscosities, ζ and η:

$$\zeta = \frac{P}{2\Delta} \tag{2.4}$$

$$\eta = \frac{P}{2\Delta e^2} \tag{2.5}$$

where

$$\Delta = [(\dot{\epsilon}_{11} + \dot{\epsilon}_{22})(1 + e^{-2}) + 4e^{-2}\dot{\epsilon}_{12}^2 + 2\dot{\epsilon}_{11}\dot{\epsilon}_{22}(1 - e^{-2})]^{1/2} \tag{2.6}$$

Hunke & Dukowicz (1997) obtained the EVP model by adding an elastic term to (2.3). The EVP model allows for a fully explicit implementation and avoids the stringent time step restriction of the VP model. The EVP model is given by:

$$\dot{\epsilon}_{ij} = \frac{1}{E}\frac{\partial \sigma_{ij}}{\partial t} + \frac{1}{2\eta}\sigma_{ij} + \frac{\eta - \zeta}{4\eta\zeta}\sigma_{kk}\delta_{ij} + \frac{P}{4\zeta}\delta_{ij} \tag{2.7}$$

where E is Young's modulus.

The elastic term, the first term on the right-hand side of (2.7), is considered to be the elastic contribution to the strain rate. The elastic term is not meant to be physically realistic but acts to regulate the VP rheology by controlling the behavior in the limit of infinite viscosity.

2.3 Thermodynamics

CICE has three different thermodynamic options. They are 1) "zero-layer" thermodynamics where the ice is fresh and does not store heat, 2) the Bitz and Lipscomb model which assumes a fixed salinity profile and 3) the "mushy" formulation where the salinity evolves. The "mushy" formulation is chosen for this project because its ability to allow salinity to evolve makes it the most realistic, and the computational penalty was acceptable for the relatively short integrations (less than one year) used in this study.

2.3.1 Temperature Updates

The conservation equation for the internal heat content is given as:

$$\frac{\partial q}{\partial t} = \frac{\partial}{\partial z}\left(\kappa\frac{\partial T}{\partial z}\right) + \omega\frac{\partial q_{br}}{\partial z} + F \tag{2.8}$$

where q is the amount of heat content used or released by the sea ice at constant pressure (enthalpy), ω is the vertical Darcy velocity of the brine, q_{br} is the brine enthalpy and F is the internally absorbed shortwave radiation. κ is the bulk thermal conductivity of the ice

and is given by a weighted average of the fixed thermal conductivities for brine κ_{br} and for ice κ_i:

$$\kappa = \phi\kappa_{br} + (1 - \phi)\kappa_i. \tag{2.9}$$

The first term on the right-hand side of (2.8) represents heat conduction. The second term represents the vertical advection of heat by gravity drainage and flushing. This equation determines the temperature of the ice.

2.3.2 Surface Forcing

CICE allows for two different methods of computing albedo and shortwave fluxes. In the CCSM3 method, albedo depends on the temperature and thickness of ice and snow and on the spatial distribution of the incoming solar radiation. See Holland *et al.* (2012) for details. The other method is a multiple scattering radiative transfer scheme that uses a Delta-Eddington approach. The Delta-Eddington method calculates some optical properties, such as albedo and absorbed flux, at each ice layer. Other optical properties, such as the extinction coefficient, are explicitly set with empirical data. This method is described in detail in Brieglab & Light (2007). The Delta-Eddington scheme is used in this project setup because it allows for melt ponds to be parameterized explicitly, while the CCSM3 method only allows for implicit melt pond parameterization. Accurate melt pond parameterization is important because it alters the heat budget of the ice.

2.3.3 Growth and Melting

Growth and melting are expressed as a product of enthalpy and change in ice thickness. At the top surface, melting is defined by:

$$q\delta h = \begin{cases} (F_0 - F_{ct})\Delta t & \text{if } F_0 > F_{ct} \\ 0 & \text{otherwise} \end{cases} \tag{2.10}$$

F_0 is the net energy flux from the atmosphere to the ice, and F_{ct} the conductive flux from the top surface to the ice interior. Therefore, if there is more flux from the top surface to

the ice interior than total energy flux from atmosphere to ice, then the growth/melting term is set to 0. This prevents unphysical ice growth on the surface.

The growth and melting at the bottom are given by:

$$q\delta h = (F_{cb} - F_{bot})\Delta t, \tag{2.11}$$

where F_{cb} is the conductive heat flux at the bottom surface, and F_{bot} is the net downward heat flux from the ice to the ocean (Maykut & McPhee, 1995).

2.4 Time Step

CICE allows the user to specify two different time steps. Δt (dt) is the thermodynamic time step and Δt_{dyn} (dt_dyn) is the dynamic time step. For global runs, a thermodynamic time step of Δt = 3600s is reasonable. Since an idealized strait with dimensions similar to those of Nares Strait is the region of interest and a much finer spatial resolution is used, a smaller thermodynamic time step must be used. A convergence study for Δt was conducted by running the model using successively smaller values from 3600s down to 240s. For time steps Δt = 300s and Δt = 240s the model was found to be near convergence, as there were negligible differences between the two runs.

To choose the appropriate dynamic time step Δt_{dyn}, the number of dynamics steps per thermodynamic time step, ndtd, must be specified.

$$\Delta t_{dyn} = \frac{dt}{ndtd} \tag{2.12}$$

Following Dumont *et al.* (2009), a dynamic time step $\Delta t_{dyn} = 0.5$. Testing for model convergence was also done for Δt_{dyn}, and the results are consistent. Furthermore, $\Delta t_{dyn} = 0.5$ satisfies the CFL condition under remapping which is:

$$\Delta t_{dyn} < \frac{min(\Delta x, \Delta y)}{2max(u, v)} \tag{2.13}$$

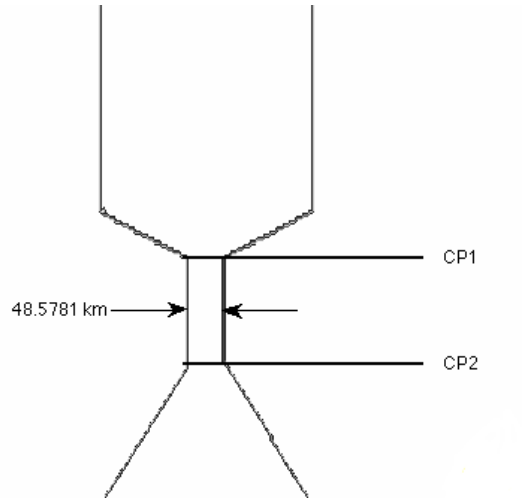

Figure 2.1: Idealized domain and locations of constriction points

Here min(Δx, Δy) is 3030m and the maximum ice velocity is always significantly smaller than 1515m/s. While this condition is always satisfied, it is not sufficient for an appropriate time step. The thermodynamic time step was found to be more important for our study.

2.5 Domain and Experimental Design

The domain is geographically and dimensionally similar to Nares Strait, opening into Lincoln Sea to the north and into Baffin Bay to the south, with dimensions of roughly 800km by 300km. The domain consists of a wide rectangular basin that converges into an approximately 48.5-km-wide channel that is 16 grid cells in width. The channel then opens back up into a wider area. There are two constriction points that are of interest in the domain. The first one, referred to as CP1, is the northernmost constriction point, while the second, CP2, is the southernmost constriction point (Fig. 2.1).

A detailed examination of the effects of changing ice cohesion e and initial ice thickness h_0 on ice bridge formation (see Chapter 3) showed that $e = 0.9$ results in stable ice bridges for all choices of h_0. Some of these form at CP1 and others at CP2. Thus, for

the numerical experiments investigating bridge disintegration, e is fixed at 0.9. In each case, the bridge is allowed to strengthen for 7 days after initial formation. It is then subjected to a variety of different atmospheric and oceanic forcings to determine their effectiveness in breaking down the ice blockage. First, the effect of temperature is tested by adding high temperature values to the range of stable bridges. Longwave radiation, shortwave radiation, wind and currents are all then tested independently. Those parameters are also tested paired with an increased temperature. Longwave radiation, shortwave radiation and temperature are tested together to study their combined effect on the bridges. Finally, a seasonal progression is conducted using one month of typical winter thermodynamic conditions, 3 months of typical spring conditions and three months of summer conditions.

Chapter 3

FORMATION

Following Dumont *et al.* (2009), a sensitivity study is conducted on the idealized domain in order to determine suitable conditions for the formation of stable ice bridges. The two varying, free model parameters are initial ice thickness h_0 and shear strength, which is determined by the variable e. The results deviate slightly from those of Dumont *et al.* (2009), primarily as a consequence of making changes to the setup to portray a more realistic scenario. The changes are detailed below.

In order to form ice bridges in the strait, certain boundary and environmental conditions must be met. Since Dumont *et al.* (2009) successfully identified a portion of the parameter space leading to such conducive conditions, we used that work as a guide. Ice density and the ocean drag coefficient are set to 905.0 kg m^{-3} and 3.24 x 10^{-3}, respectively, as in Dumont *et al.* (2009). A constant 10m/s northerly wind is applied uniformly over the domain. This represents the strong wind conditions found in Nares Strait. Coriolis force and thermodynamics are modeled explicitly. Thermodynamic parameter values representative of winter conditions were chosen (Table 3.1). Initially, the entire domain is covered with ice with uniform concentration (100% ice cover) and uniform thickness (h_0). At the northern boundary, ice thickness is held constant at h_0. Thus ice is advected from the north into the domain by the wind, while the southern boundary is open to allow ice to flow out of the domain.

All formation simulations are run for 31-46 days. In order to be classified as a stable ice bridge, the ice edge must not move over a 14-day period. e and h_0 ranges are

Table 3.1: Typical Winter Values

Parameter	Value
Air Potential Temperature	-20°C
Air Temperature	-20°C
Specific Humidity	0.0006kg/kg
Incoming Longwave Radiation	180W/m^2
Incoming Shortwave Radiation	0W/m^2
Latent Heat Flux	0W/m^2

chosen based on the ranges used by Dumont *et al.* (2009). The range for e used by Dumont *et al.* (2009) is 1.2 to 2.0. Due to the changes made in this set-up, including the addition of thermodynamics, Coriolis and incoming ice at the northern boundary, values of 1.4 and higher produce unstable bridges or no bridges at all. Therefore, the model is then tested with e values lower than 1.4 by 0.1 increments. The lowest value is $e = 0.5$. For this value, stable ice bridges form for all tested initial ice thicknesses, and lower values of e will only have stronger cohesion. h_0 ranges from 0.5m to 3.0m, which reflects reasonable values found in Nares Strait and is comparable to the ranges used by Dumont *et al.* (2009).

Bridges form at both CP1 and CP2. Figure 3.1 shows a bridge formed at CP1. The ice bridge is clearly defined as an arch delineating higher ice thickness as shown by the color contour. Dark blue represents an area of open water with no ice. This particular bridge is formed with an initial ice thickness $h_0 = 0.75$m and a cohesion parameter of $e = 0.9$ (a mid-range value). Figure 3.2 shows a bridge formed at CP2. This bridge is formed with an initial thickness of $h_0 = 2.0$m and a cohesion parameter of $e = 0.9$. For some parameter combinations, bridges form unstably or do not form at all.

At its smallest value of 0.5, e produces stable ice bridges at CP2 irrespective of the initial ice thickness h_0. On the other hand, an e value of 1.4, at any thickness, either does not produce a stable bridge or does not produce a bridge at all. Note that the location of the ice bridge is dependent upon initial ice thickness h_0. Smaller values of h_0 produce

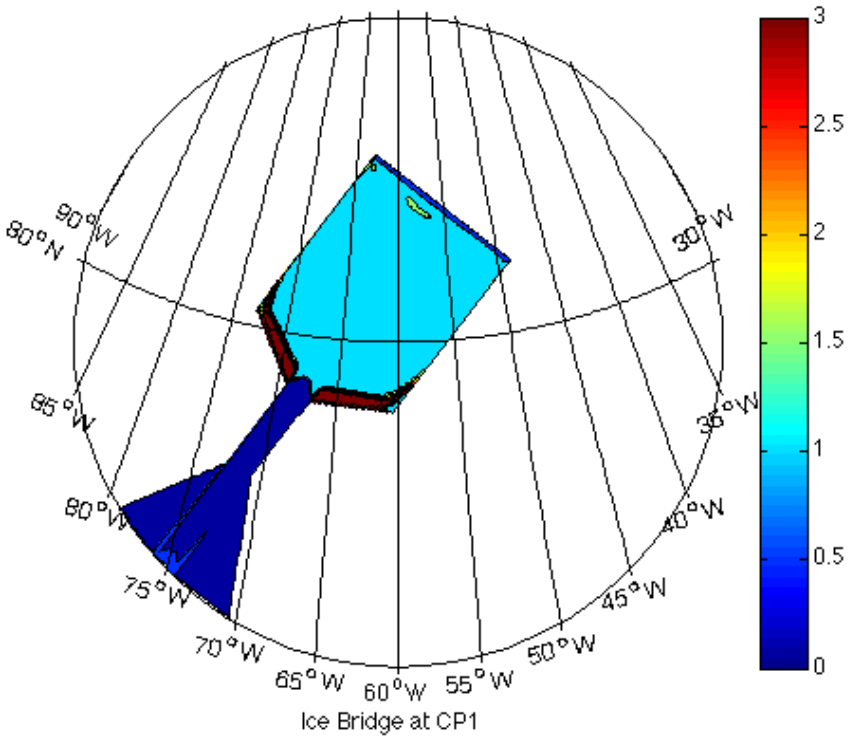

Figure 3.1: Ice bridge formed with an initial ice thickness of 0.75m and a cohesion parameter of $e = 0.9$ with -20°C air temperature and longwave radiation of 180W/m^2. Color represents ice thickness in meters.

bridges at CP1. Recall that ice of the same thickness as the initial thickness over the strait is entering through the northern boundary. Hence, when e is 0.7-1.0 and h_0 is 0.75m, the mixture of ice cohesion and pressure from incoming ice is sufficient for ice bridge formation at CP1. Low e values cause ice to be more cohesive. The increased cohesiveness promotes stronger ice that can withstand the stress from the incoming ice at the northern boundary. This causes bridges to form at CP2 as opposed to CP1.

As expected, ice bridges do form at small initial thicknesses when the value of e is low enough. When $e \leq 0.9$, stable bridges form when $h_0 = 0.5$m. When larger values of e were used, $e = 1.1$-1.4, no stable bridges were formed at CP1. Also, when $e = 1.2$ -1.4

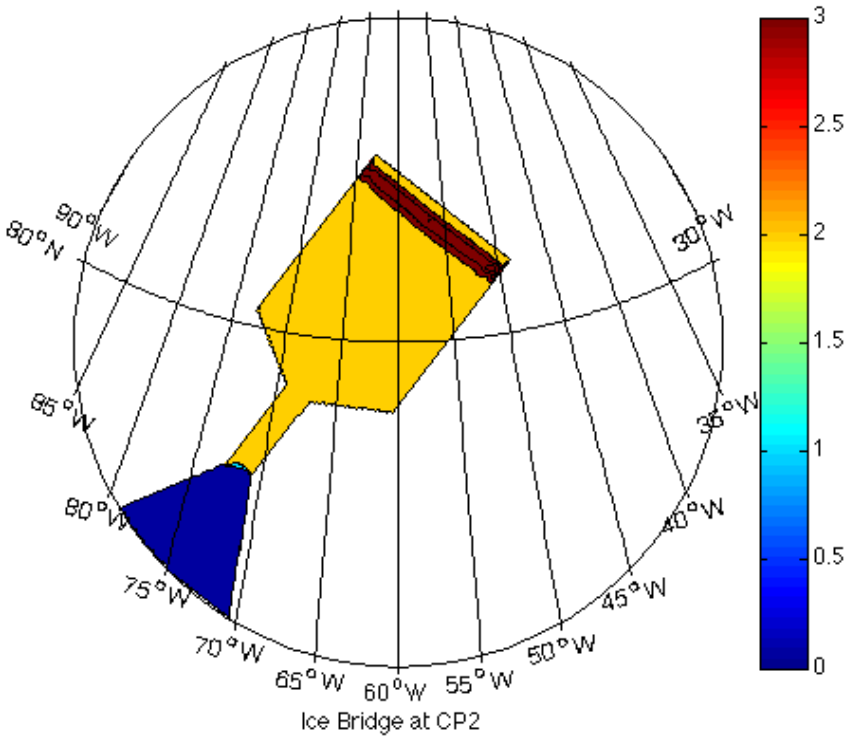

Figure 3.2: Ice bridge formed with an initial ice thickness of 2.0m and a cohesion parameter of $e = 0.9$ with -20°C air temperature and longwave radiation of 180W/m^2. Color represents ice thickness in meters

and $h_0 = 2.5$m, unstable bridges were formed at CP2. This is because there is not enough cohesion for initial/incoming ice that thick. The pressure from the incoming ice is likely too much for ice that has such low cohesion. On one occasion, a stable bridge formed in between CP1 and CP2. In this special case, $h_0 = 0.5$m and $e = 0.7$. Note that bridges formed with the preceding and succeeding values of e at the same initial thickness form at CP1 and CP2, respectively. The full scope of results from the sensitivity study of ice bridge formation is shown in Figure 3.3.

As our aim is to study the destruction of the ice bridges, a cohesion parameter of e=0.9 is chosen for all following experiments. It has the advantage of permitting stable

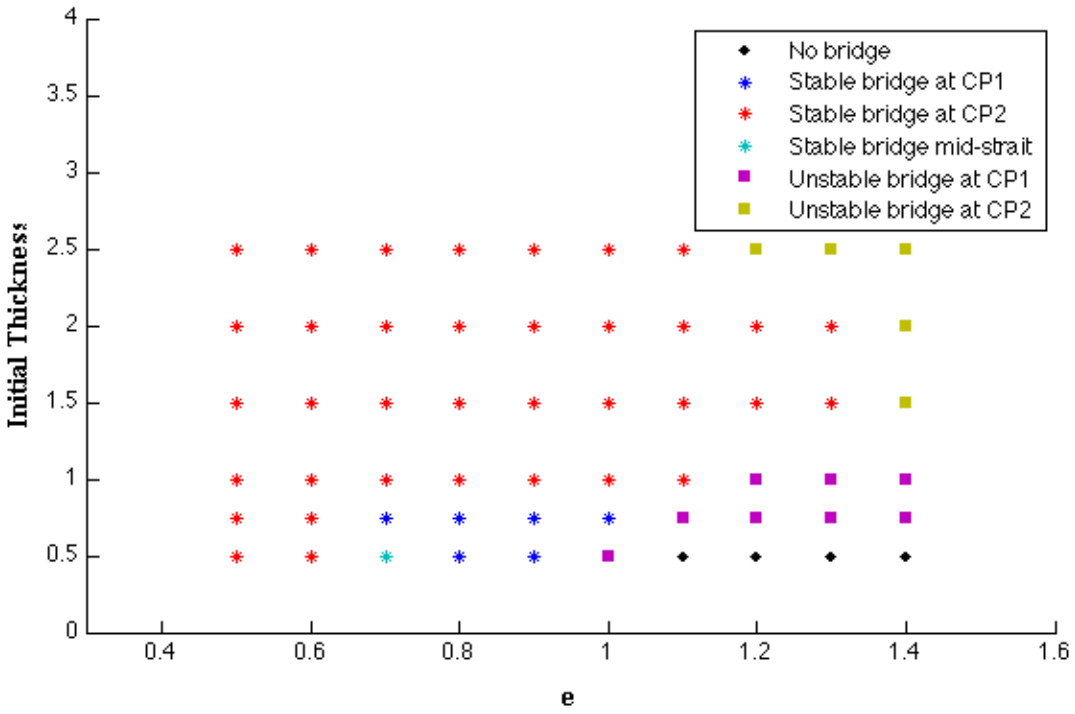

Figure 3.3: Results of the sensitivity study. Six behaviors are observed: no bridge (black diamond), stable bridge at CP1 (blue asterisk), stable bridge at CP2 (red asterisk), stable bridge midway between the two constriction points (teal asterisk), unstable bridge at CP1 (magenta square) and unstable bridge at CP2 (dark yellow square)

bridge formation over the entire range of initial thicknesses h_0.

Chapter 4

RESULTS AND DISCUSSION

4.1 Destruction Scenarios

The collection of model runs demonstrates that there are three different ways the ice bridges break up. The first is the "complete collapse" (Figure 4.1). In this scenario, the defined ice arch completely collapses, allowing for ice to flow freely through the constricted part of the domain. This scenario only occurs for bridges formed at CP1 or those that form at CP2 but melt to CP1 before breaking. The second scenario is the "flowing collapse" (Figure 4.2). This scenario occurs with bridges formed at CP2. The defined ice arch weakens and allows ice to flow into the bottom of the domain. The remnant of the ice arch is visible as the leading ice edge of the flowing ice. The final scenario is the "slow leak" (Figure 4.3). Small pieces of ice break off around the defined ice arch. Due to the Coriolis effect, these pieces are deflected to the right of the flow and pile on the western edge of the strait. This only occurs for ice bridges formed from high initial ice thicknesses h_0. These bridges originally form at CP2 but melt to CP1. Then, due to the high stress from the incoming thick ice, little pieces of ice break off. Often times, the ice arch maintains its shape, however thinning, as it recedes north. A complete collapse of the defined ice arch never occurs in the cases examined here. However, ice is allowed to escape along the western edge.

4.2 Air Temperature

Constant extreme air temperature values of 20°C and 30°C are imposed on a stable ice bridge to isolate the effects of temperature. In these scenarios, shortwave radiation is set

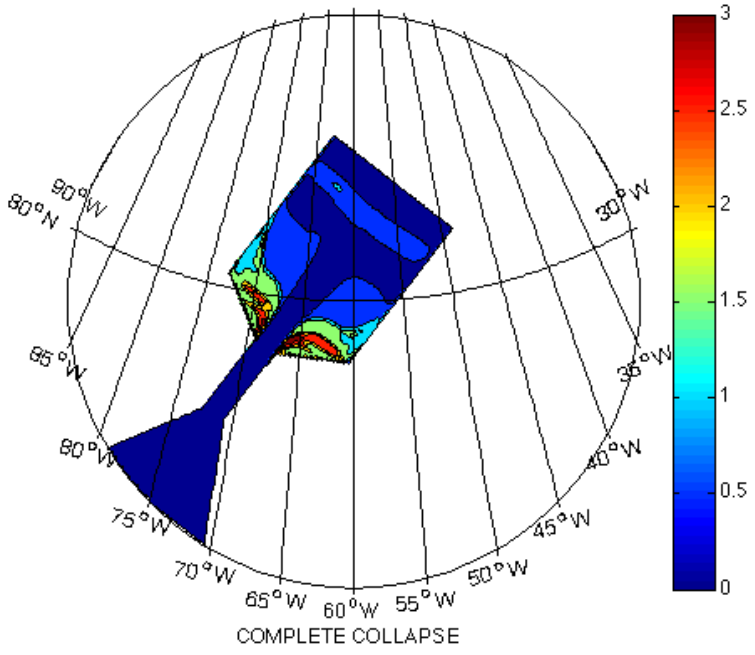

Figure 4.1: Complete Collapse scenario. The color bar represents ice thickness in meters.

to zero, and longwave radiation is set to the winter normal value of 180W/m^2, retaining the values used during the formation of the bridges. Initial thicknesses h_0 of 0.5m to 3.0m are tested. The bridge formed at the respective initial thickness h_0 is allowed to strengthen for 7 days before the temperature change is implemented.

At both of the extreme temperatures tested, 20°C and 30°C, all ice bridges break up within eight months, regardless of initial thickness h_0. There is a steep drop in the time to breakup from 20°C to 30°C, particularly at higher initial thicknesses h_0 (Figure 4.4). Generally, as the initial thickness h_0 increases, the number of days the bridge persists increases. One exception are the $h_0 = 1.0$m bridges. The $h_0 = 1.0$m bridge under both 20°C and 30°C air temperature take less time to break than the 0.75m bridges under the same air temperature. The $h_0 = 1.0$m bridge also takes less time to break than the 0.5m bridge under 30°C. This result can be explained by the location of the bridge: The $h_0 = 1.0$m bridge forms

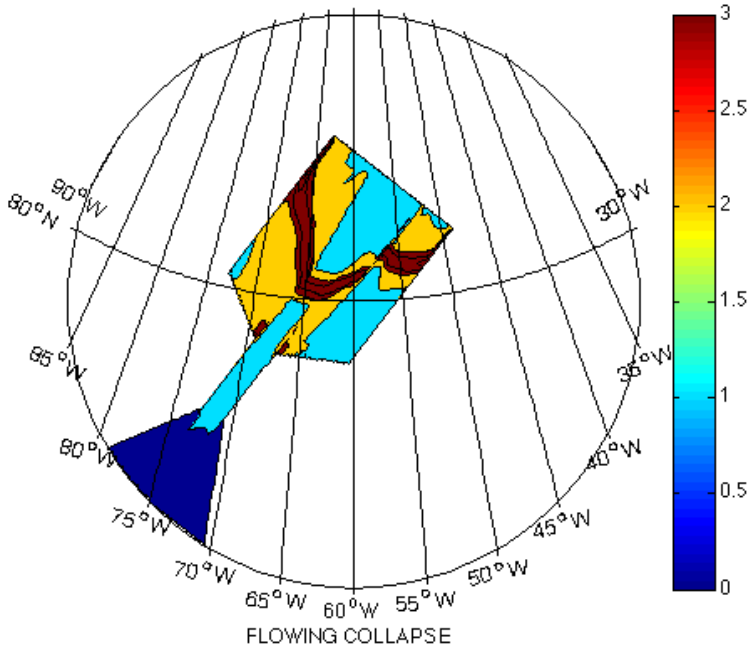

Figure 4.2: Flowing Collapse scenario. The color bar represents ice thickness in meters.

at CP2. It is the thinnest bridge to form at CP2 and therefore, the weakest. Whereas, the $h_0 = 0.75$m bridge is the thickest and strongest bridge to form at CP1.

Figure 4.5 shows a bridge with an initial thickness of 0.75m at day 1 and day 31. In this scenario, only air temperature is being increased (30°C), as the longwave radiation value is still the same as when the bridge was formed (180W/m^2). The bridge completely collapses relatively fast, lasting only 31 days. The break-up process is similar for all bridges tested with 20°C air temperature, except for the one formed with $h_0 = 3.0$m. The $h_0 = 3.0$m bridge under 20°C air temperature takes over 100 days less to break than the $h_0 = 2$m bridge under the same air temperature. This bridge also persists only 20 days longer than the same bridge under 30°C air temperature forcing. This is because the ice advected into the domain at the northern boundary is equal to h_0. The 3.0m incoming ice does not melt fast enough under 20°C air temperature, so there is significant stress on the bridge from the

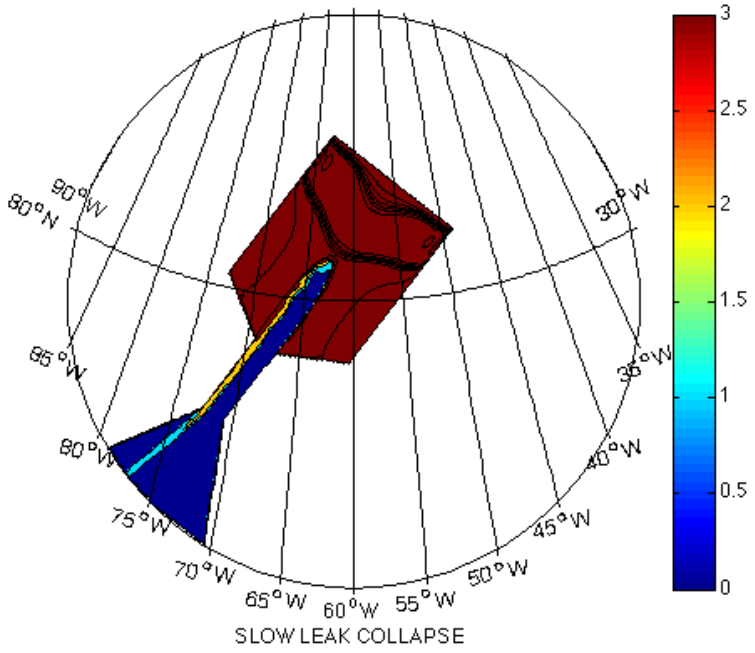

Figure 4.3: Slow Leak scenario. The color bar represents ice thickness in meters.

thick ice. Thus, the bridge breaks sooner. This is not seen when the air temperature is 30°C because the high air temperature melts the bridges and incoming ice too fast and becomes too dominant.

With an incoming longwave radiation value of 180W/m^2 and an air temperature of 10°C, only $h_0 = 0.5$m and 0.75m bridges break up within eight months. The bridges in these scenarios take 166 and 221 days to break up, respectively. No bridges, regardless of initial thickness h_0, break up within 8 months when the air temperature is 0°C. Since typical summertime air temperatures in Nares Strait range from 0°C to 10°C, other factors than air temperature must be critical for bridge destruction.

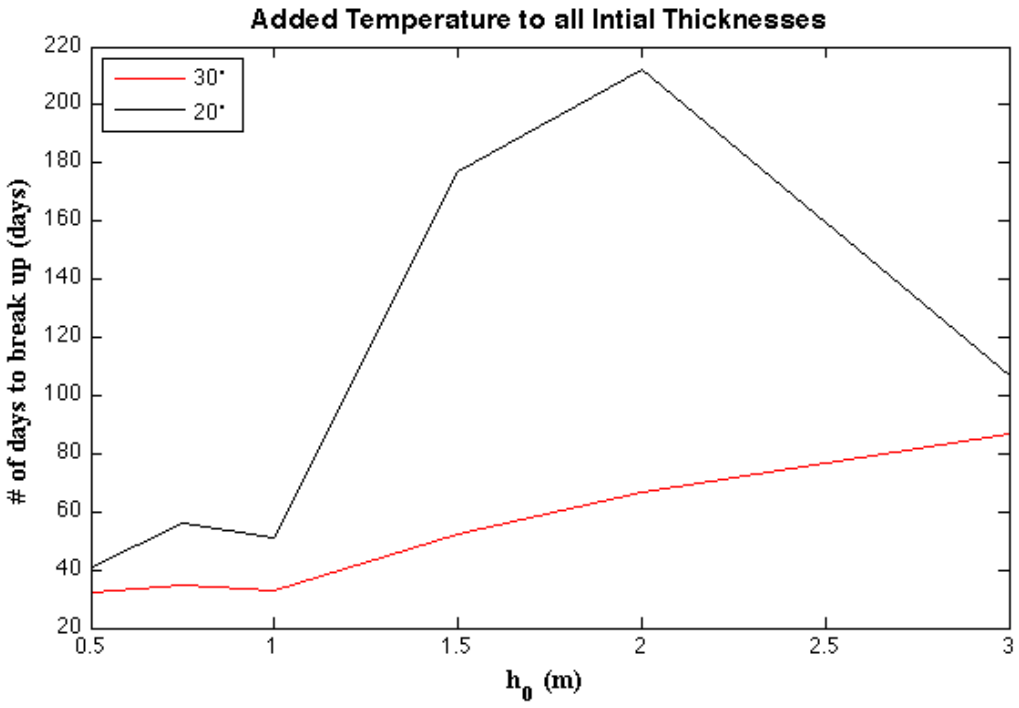

Figure 4.4: Extreme air temperature experiments

4.3 Radiative Forcing

4.3.1 Longwave Radiation

Observations at Alert from NOAA's Earth System Research Laboratory in 2013 show incoming longwave radiation for Nares Strait ranging from around 115 to 350W/m^2. In order to isolate its effects on stable ice bridges, incoming longwave radiation is set to a high value of 280W/m^2. These tests are run with no shortwave radiation and a realistic air temperature of 0°C. A bridge formed with the smallest initial thickness $h_0 = 0.5$m is tested first. Under these conditions, the ice bridge does not break up within 248 days, or 8 months. In Figure 4.6, it is evident that ice is being advected into the domain at the north and is starting to pile up and thicken. The high longwave radiation value of 280W/m^2, however, is not strong enough to weaken the bridge under the stress of the incoming ice. Thus, the bridge

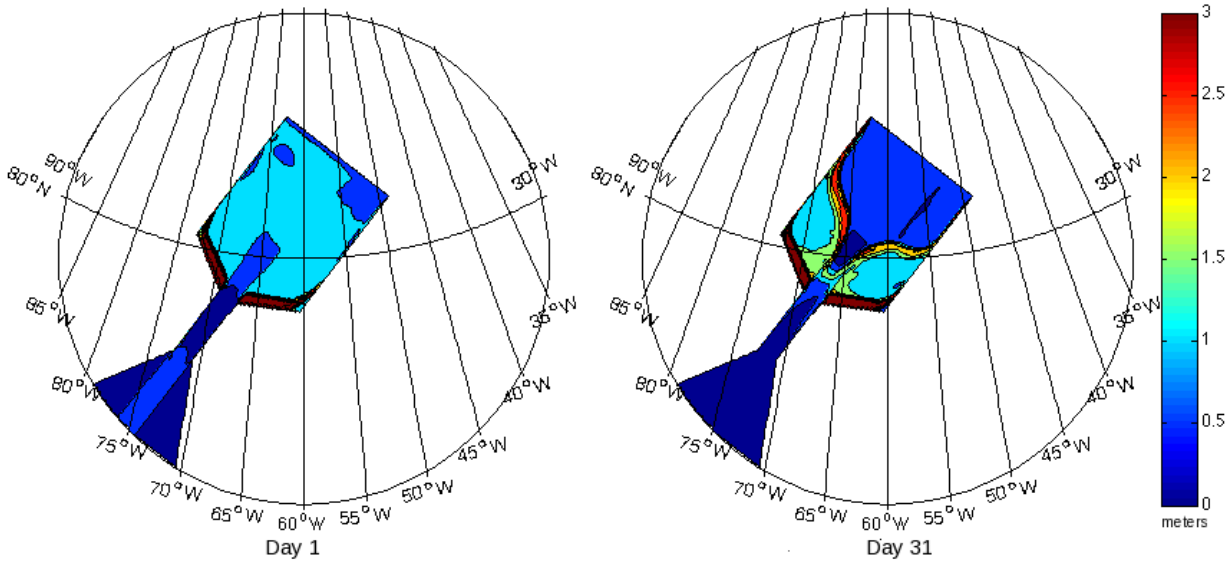

Figure 4.5: Ice bridge formed with an initial ice thickness of 0.75m and longwave radiation of 180W/m^2 collapses under 30°C air temperature. Color represents ice thickness in meters.

persists and even appears to be reinforced by another arch like ice structure further north. This suggests that incoming longwave radiation alone cannot be the driving mechanism for the destruction of ice bridges. Therefore, testing this scenario for other initial thicknesses h_0 was not pursued.

4.3.2 Shortwave Radiation

Next, the effects of shortwave radiation are isolated using high values that would be consistent with summertime conditions. A total incoming shortwave radiation value of 280W/m^2 is used along with no longwave radiation and an air temperature of 0°C. Figure 4.7 shows a bridge formed with an initial thickness $h_0 = 0.5$m on day 7 and day 248. After 248 days, the bridge has not been destroyed. Again, it is reinforced by the incoming ice. Thus, shortwave radiation alone also does not suffice for the destruction of ice bridges, and no further testing is done for bridges formed with higher initial thickness h_0 values.

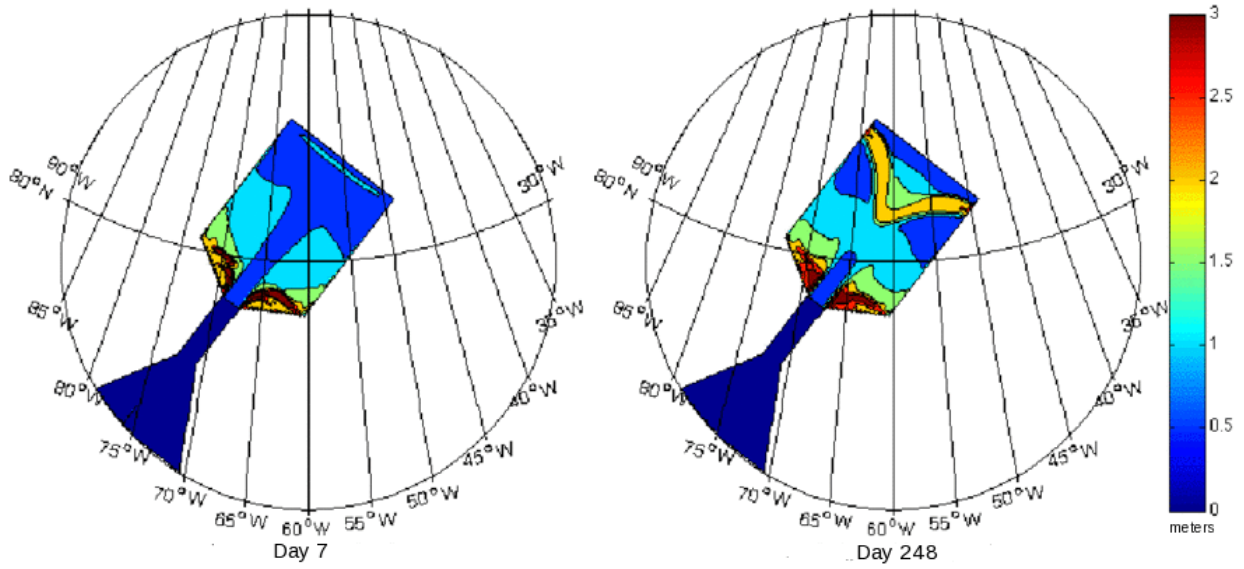

Figure 4.6: 280W/m^2 of incoming longwave radiation added to a stable 0.5m thick bridge

Interestingly, the ice collected in the northern part of the domain is thicker when shortwave radiation is tested than when longwave radiation is tested (despite being the same value). Comparing the scenarios in Figures 4.6 and 4.7, shortwave radiation does not cause as much melting of the incoming ice, resulting in thicker ice in the northern part of the domain. This is because incoming shortwave radiation is scaled by the albedo of the ice, whereas longwave radiation is not. However, the bridge in the shortwave scenario recedes further north than the bridge in the longwave scenario. The ice advected into the strait in the shortwave scenario is being melted less upon entering than the incoming ice in the longwave scenario. This causes the ice in the north to pile up and thicken. In turn, this adds more stress to the bridge, causing it to recede further and essentially weaken. Both scenarios are ineffective in destroying the ice bridges. However, longwave radiation is more effective in melting the incoming ice and bridge, whereas, the shortwave scenario is more effective in weakening the bridge due to the thicker ice exerting stress on the bridge.

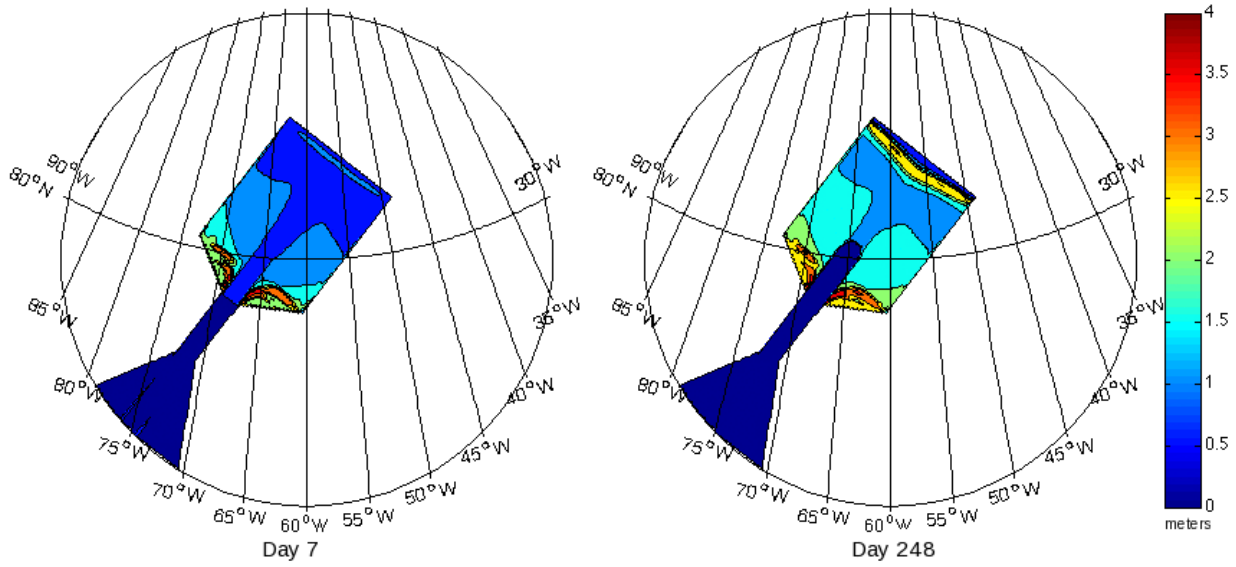

Figure 4.7: 280W/m^2 of incoming shortwave radiation added to a stable 0.5m thick bridge

4.4 Longwave Radiation and Air Temperature

Combinations of a range of incoming longwave radiation values and increased air temperatures are tested to observe their combined effect on stable ice bridges. Incoming longwave radiation values range from 180 to 300W/m^2 and temperature ranges from 0 to 30°C. h_0 also ranges from 0.5 to 3.0m. There is no shortwave radiation. First, the entire range of h_0 and longwave radiation is tested at 30°C. Figure 4.8 shows the number of days the bridges persist as a function of h_0. All bridges, regardless of h_0, break up within 248 days. In fact, all break up in under 90 days. The pattern is very consistent. The thicker the initial ice is, the longer the bridge takes to break up, with the exception of the $h_0 = 1.0$m bridge (see the discussion in Section 4.2). Also, the smaller the incoming longwave radiation is, the longer the bridge persists. This predictable pattern is not apparent when air temperature is 20°C or lower, suggesting that the air temperature of 30°C is past a critical threshold for weakening and destroying the ice bridges.

Figure 4.9 shows the range of longwave radiation tested at 20°C. All bridges,

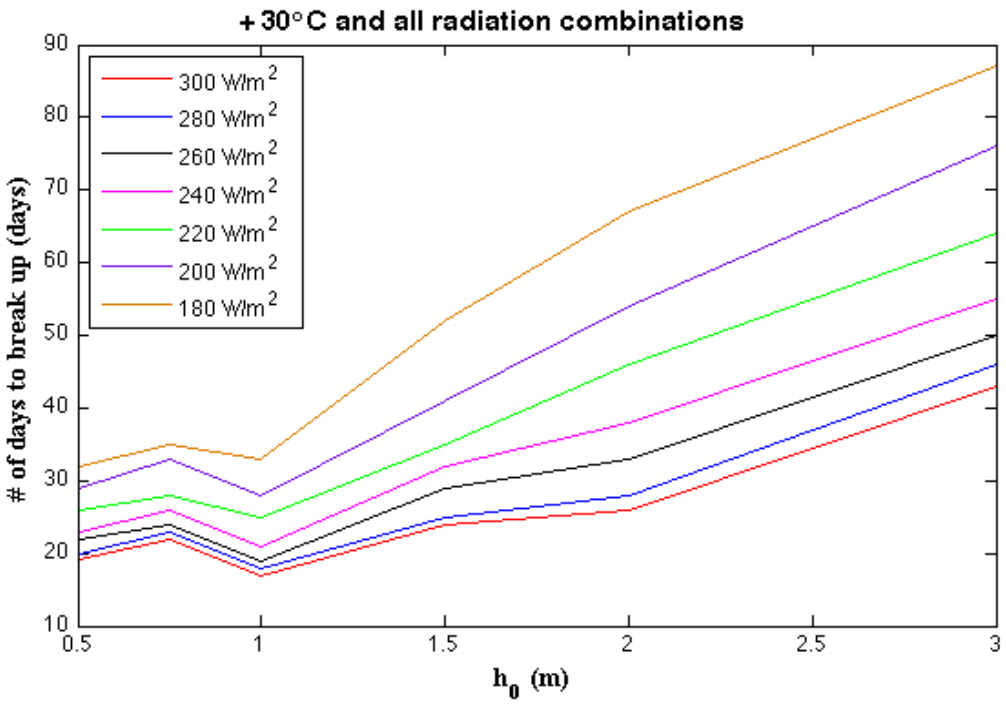

Figure 4.8: Range of longwave radiation and h_0 values at 30°C

regardless of thickness and longwave radiation value, break up within 248 days, or roughly 8 months. The lowest longwave radiation value tested, 180W/m^2, takes 212 days to break up when $h_0 = 2.0$m. However, when $h_0 = 3.0$m, it takes only 107 days. This decrease in days with respect to an increase in h_0 is also seen when longwave radiation is set to 200W/m^2. However, the decrease is significantly less dramatic. The $h_0 = 3.0$m bridge, persisting 137 days, collapses sooner than the $h_0 = 2.0$m bridge, persisting 142 days.

In most cases, increased radiation leads to less stable ice bridges, as it enhances the melting and weakens the ice. In most cases, bridges of thicker and hence stronger ice persist longer. The two outlier scenarios ($h_0 = 3.0$m with 180W/m^2 and with 200W/m^2 radiative forcing) demonstrate, however, that the physics is more complex. The primary factor controlling bridge disintegration is the balance between the strength of the ice bridge

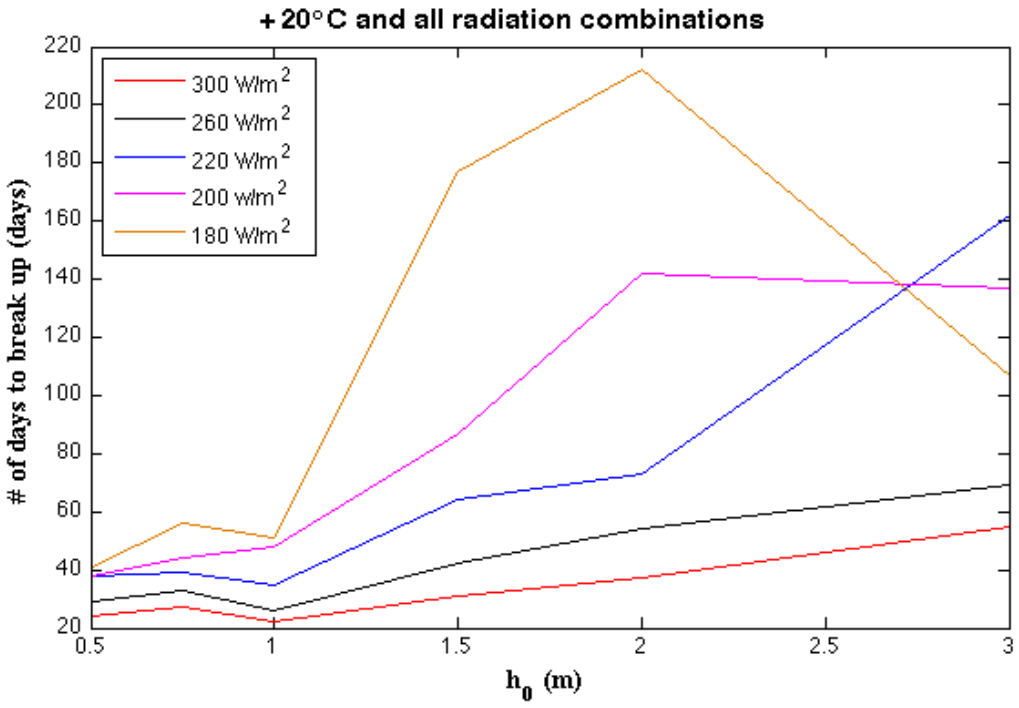

Figure 4.9: Range of longwave radiation and h_0 values at 20°C

and the stress imposed on it by the ice pushed down-strait by the wind forcing. Conditions that lead to strong bridges - thick ice, little melting - are also conducive to high stress from the incoming ice, which is also stronger. With the low radiative forcing and high ice thickness combinations the balance shifts, so that the increased stress overcomes the increased bridge strength. This is why the bridges in these outlier scenarios disintegrate before the thinner $h_0 = 2.0$m bridge with the same radiative forcing.

Finally, despite the thickness increase, 1.0m ice bridges take less time to break than 0.75m ice bridges, under both air temperatures. This is consistent with the results from previous sections. All other experiments in this group follow the regular pattern found in the 30°C air temperature scenario (Figure 4.9).

4.5 Shortwave Radiation and Air Temperature

Observations at Alert from NOAA's Earth System Research Laboratory in 2013 show incoming shortwave radiation for Nares Strait ranging from around 0 to 520W/m^2. Thus four representative values of incoming shortwave radiation, 100, 200, 280 and 400W/m^2, are tested under an air temperature of 20°C on stable bridges at a variety of initial thicknesses h_0. The largest shortwave radiation value, 400W/m^2, causes the bridges to break up within eight months, regardless of initial thickness h_0. With a shortwave radiation value of 280W/m^2, h_0 = 1.5m bridges do not break up within 8 months. The same is true for h_0= 1.0m and 1.5m bridges with a shortwave radiation value of 200W/m^2. Finally, when the shortwave radiation is 100W/m^2, only h_0 = 2m and 3m bridges are destroyed within eight months. Figure 4.10 shows the time to disintegration for each scenario.

Generally, destruction time decreases as shortwave radiation increases. Also, all of the tested shortwave values at all initial thicknesses up to h_0 = 1.5m result in longer time to destruction with increasing initial thickness h_0. However, the destruction time decreases as h_0 exceeds 1.5m. The h_0 = 2.0m scenarios have 2.0m thick ice being advected in at the northern boundary. This thicker ice is more resistant to the incoming shortwave radiation than 1.5m thick ice due to an increase in albedo with the increase in thickness. There is less melting of the incoming ice. In turn, there is a greater pile up of ice in the north which adds stress on the ice bridge. Thus, it collapses sooner than the h_0 = 1.5m scenario.

The same could be true for the scenarios where h_0 = 3.0m. The destruction time is much lower here than in any of the other scenarios, including those with h_0 at its lowest value of 0.5m. These bridges break following the "slow leak" scenario described in Section 4.1. When the pieces of ice break off at CP2 and the ice bridge edge begins to recede north, the pieces break off unevenly. This allows for even more ice to leak along the western edge.

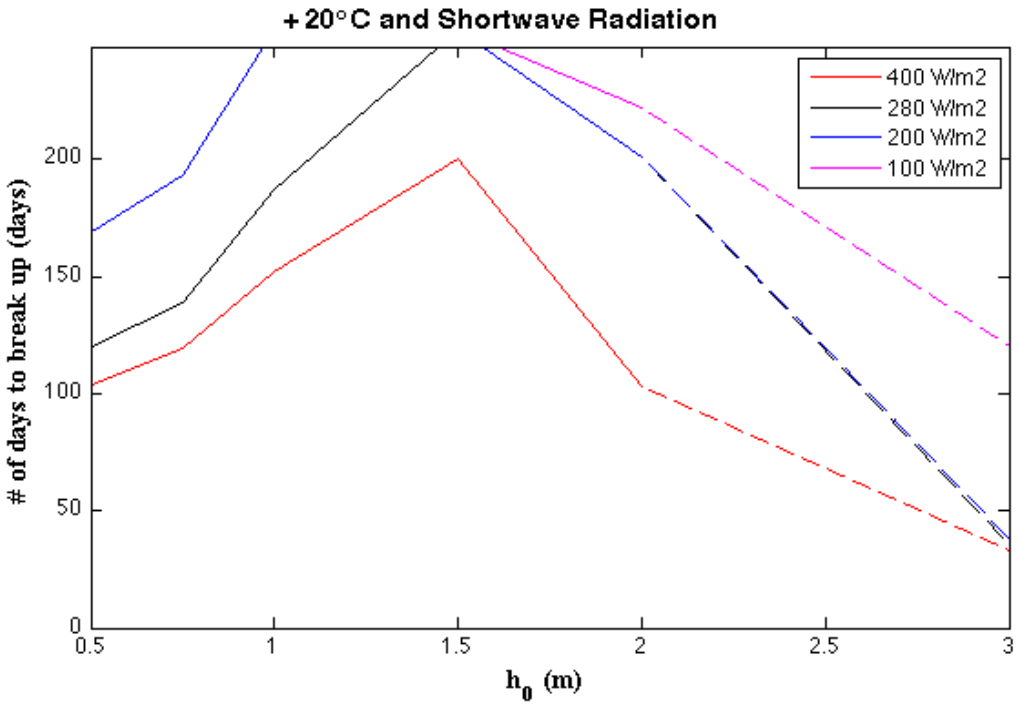

Figure 4.10: Range of shortwave radiation and h_0 values at 20°C. Since h_0 = 2.5m was omitted from the study and the results at h_0 = 3.0m are much lower that at other initial thicknesses, the lines are differetinated by being dashed. The graph is cut at 250 days to show that certain bridges took longer than 8 months to collapse.

4.6 Longwave Radiation, Shortwave Radiation and Air Temperature

Two values for each of longwave radiation, shortwave radiation and temperature are combined to test stable ice bridges at three different ice thicknesses h_0. Values for longwave radiation are chosen to represent a moderate value and a high value, 240 and 300W/m^2, respectively. The same is true for the shortwave radiation values of 100 and 200W/m^2. Finally, the two temperatures tested were 0 and 10°C. All bridges, regardless of initial thickness h_0, break up within 8 months. The combinations are summarized in Table 4.1 and the results are shown in Figure 4.11.

The 0.5 and 1.0m bridges take the longest to break under combination A, which has

Table 4.1: Longwave, Shortwave and Temperature Combinations

Combination Name	Longwave Radiation	Shortwave Radiation	Temperature
A	240W/m^2	100W/m^2	0°C
B	240W/m^2	200W/m^2	0°C
C	300W/m^2	100W/m^2	0°C
D	300W/m^2	200W/m^2	0°C
E	240W/m^2	100W/m^2	10°C
F	240W/m^2	200W/m^2	10°C
G	300W/m^2	100W/m^2	10°C
H	300W/m^2	200W/m^2	10°C

the lowest radiation values and temperature. This is expected as this combination features the least amount of incoming heat. Conversely, these bridges under combination H take the least time to break, as this combination features the most incoming heat. See Figure 4.11. The 0.5m and 1.0m bridges under combinations E and F (low longwave radiation, high temperature) take longer to break than combinations C and D (high longwave radiation, low temperature).

The bridges that are under combinations that have high longwave radiation values and 0°C air temperature (C and D) break before those with lower longwave radiation and a higher air temperature (E and F). This suggests that temperature is not the leading mechanism in breaking these bridges, which is consistent with the results in Sections 4.4 and 4.5. Bridges under combinations where the longwave radiation is at its highest take about the same time to break for both shortwave radiation values, regardless of air temperature. This suggests that if longwave radiation is high, then shortwave radiation differences are negligible. If longwave radiation is low, temperature and shortwave radiation effects are similar. High longwave radiation is necessary for quick break-up; adding a higher temperature cuts survival time in half.

h_0 = 3.0m ice bridge behavior under these combinations is different and even

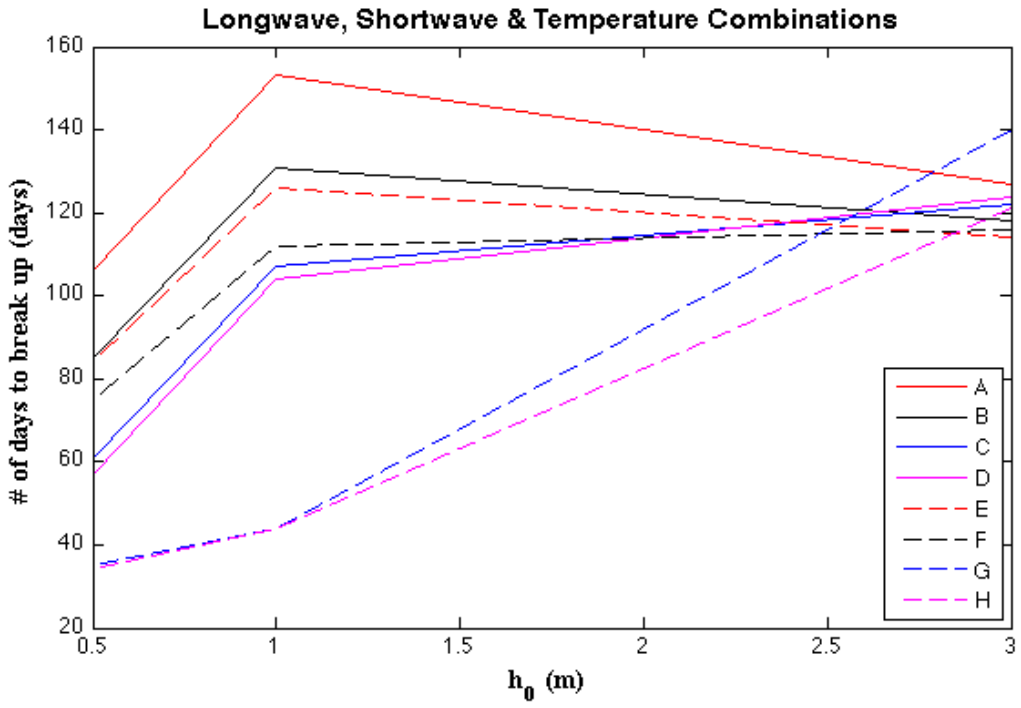

Figure 4.11: Longwave, Shortwave and Temperature Combinations at h_0 = 0.5m, 1.0m and 3.0m

counterintuitive. Combination A does not take the longest to break up at this ice thickness, despite it having the least amount of incoming heat. Also, the combination in which the bridge breaks the fastest is not the one with the most incoming heat (H). Combination E, which has the least amount of radiation at an air temperature of 10°C, takes the least amount of time to break up. The range of break-up times across all scenarios is very small, with seven of the results within 13 days of each other and the last one (G) only another 13 days longer (Table 4.2). The interplay between stronger bridges and stronger stress from the inflowing ice results in little variation in bridge lifespan among the scenarios. This suggests that the most critical factor controlling bridge breakup here is initial thickness h_0.

Table 4.2: 3.0m Bridge - Longwave, Shortwave and Temperature Combinations Results

SW Radiation, Temp.	100W/m^2, 0°C	200W/m^2, 0°C	100W/m^2, 10°C	200W/m^2, 10°C
LW Radiation 240W/m^2	"A" 127 days	"B" 118 days	"E" 114 days	"F" 116 days
LW Radiation 300W/m^2	"C" 122 days	"D" 124 days	"G" 140 days	"H" 121 days

4.7 Wind

The constant, along strait wind is varied from 5 to 20m/s in 5m/s increments at h_0 values of 0.5m, 1m and 3m. In these scenarios, longwave radiation is a constant value of 300W/m^2 and shortwave radiation is constant at 100W/m^2. 0 and 10°C air temperatures are used. The wind speed in the preceding sections is a constant 10m/s. When wind is changed to a constant 15 and 20m/s, the bridge is destroyed within one day. While strong winds like this have been observed in Nares Strait, they typically do not last continuously with that magnitude for 24 hours. Thus, the detailed testing of the effect of wind is studied through using a constant wind of 5m/s. Since the imposed stress is reduced, the expected result is that bridges last longer under weaker winds. This is born out by the $h_0 = 0.5$ and 1.0m bridges. When air temperature is 0°C the $h_0 = 1.0$m bridge does not break up within 8 months (Figure 4.12). Interestingly, when shortwave radiation is increased to 200W/m^2 this bridge does break within eight months. This highlights the influence of shortwave radiation.

Once again, the situation is different for thick bridges. Both of the $h_0 = 3.0$m bridges take significantly less time to break with 5m/s wind than 10m/s wind. When the wind is 10m/s, more thick ice is being advected into the strait than when wind is 5m/s. The larger amount of thick ice is reinforcing the bridge, making it last longer. When less thick ice is advected in, it is not enough to reinforce the bridge and adds stress to the bridge, causing it to crumble. The $h_0 = 3.0$m bridges appear to have a threshold of how much thick ice can enter before either reinforcing the bridge or destroying it. These bridges, with 5m/s wind, also take less time to break than the 0.5 and 1.0m bridges at both 5 and 10m/s. See Figure

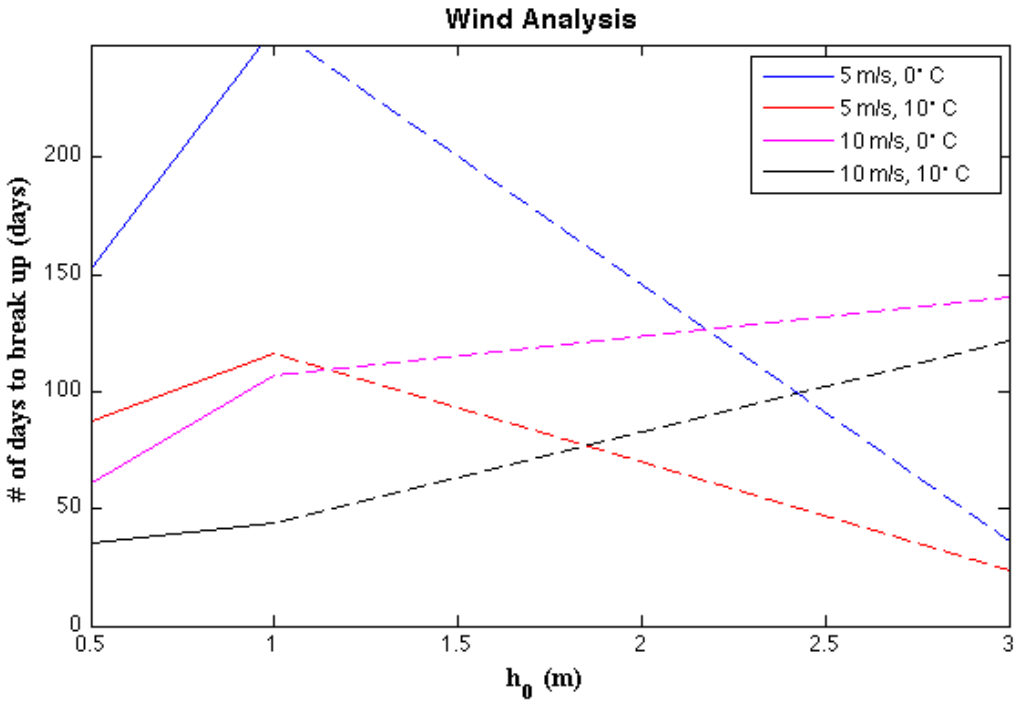

Figure 4.12: Wind analysis, varied with temperature and initial thickness. Shortwave radiation is held at 100W/m^2.

4.12.

4.8 Currents

Like wind, constant, down-strait currents have a significant effect on ice bridges. Currents are added to a base simulation to test their effect on stable 1.0 and 3.0m ice bridges. Constant values for shortwave radiation, longwave radiation and temperature of 100W/m^2, 300W/m^2 and 0°C, respectively, are used to isolate the currents effects. First, 0.25 and 1.0m/s currents are tested with a wind speed of 10m/s. The 1.0m bridges took 16days and 1 day, respectively, to break. In order to isolate the currents effects better, wind is then set to 5m/s. Currents that are 0.5-1.0m/s take 1 or 2 days to break the 1.0m bridge. Under currents that are 0.25-0.35m/s, the 1.0m bridge lasts for a more realistic length of

time. Finally to isolate the effect of the current, the wind is stopped completely. However, the results for 0.5-1.0m/s are the same: only one or two days to destroy the bridge. For comparison, a 1.0m bridge under the same thermodynamic conditions survives for about the same length of time with a 0.30m/s current and no wind as with no current and constant 10m/s wind.

The $h_0 = 3.0$m bridges behave differently than the $h_0 = 1.0$m bridges. 3.0m bridges are tested with 0m/s wind. 0.75-1.0m/s currents take 1 or 2 days to break up the bridge. 0.25-0.50m/s currents take significantly more time to break the bridges at this thickness. The 1.0m bridges take less time to break as the current speed increases. This pattern is not seen with the 3.0m bridge (Figure 4.13). In fact, as the current decreases, the amount of time to break the bridge actually decreases. For instance, a 0.25m/s current actually takes less time to break the bridge 3.0m bridge than the 0.50m/s current. This is comparable to the results from the wind analysis where 5m/s wind scenarios take less time to break the 3.0m bridges than 10m/s wind scenarios. This again reinforces the idea that there is a threshold ice thickness separating regimes where the relative importance of environmental factors on bridge strength and on imposed stress changes. It also supports the idea that ice entering the strait can act either to reinforce the bridge or to weaken it.

Regardless of initial thickness, current speeds of 0.75 and 1.0m/s have an immense effect on the bridges and break them within only 1-2 days. Current speeds of this magnitude are seen in Nares Strait observations. So it is important to remember that this model setup imposes constant current speeds in one direction. E.g., there is no tidal signal. The stress exerted by stationary ice on surface ocean currents is also not modeled here

4.9 Seasonal Progression

A seasonal progression is conducted from winter to summer. The purpose of a seasonal progression is to simulate a realistic time period and duration of bridges in Nares Strait. All of the bridges in this study are formed under winter conditions. Because of

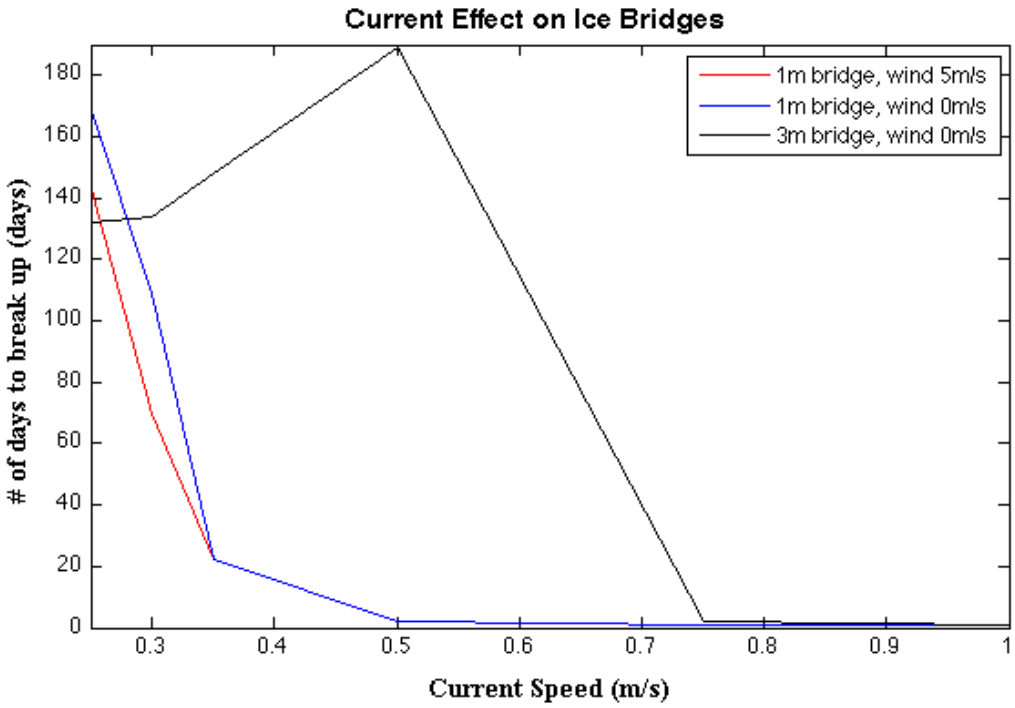

Figure 4.13: Currents Effect on Ice Bridges

that, there is only one month of winter conditions in the seasonal progression, in addition to the 7-day strengthening after formation. Then three months of spring conditions and three months of summer conditions are modeled. Air temperature and radiation values are taken from averages of observations at Alert from NOAA's Earth System Research Laboratory. The parameter values are shown in Table 4.3.

Table 4.3: Seasonal Progression Results

Season	Longwave Radiation	Shortwave Radiation	Temperature
Winter	180W/m^2	0W/m^2	-20°C
Spring	200W/m^2	100W/m^2	-10°C
Summer	280W/m^2	200W/m^2	5°C

A seasonal progression is done for h_0 = 0.5m, 1.0m, 1.5m, 2.0m and 3.0m. The

0.5m bridge takes 152 days to break, which is 28 days into Summer. Thus, it breaks around June 28. The rest of the duration dates are similar (Figure 4.14). The 1.0m bridge takes slightly less time to break than the 0.5m bridge, which is consistent with the temperature and radiative forcing sensitivity results from Sections 4.2 and 4.4. The 3.0m bridge breaks up the soonest. This is also consistent with previous results. All of the bridges break in the model's late June or early July, which is reasonably realistic. The $h_0 = 2.0$m bridge takes the longest to break. Under this seasonal progression, it would seem that initial ice thickness, h_0, is less of a factor than in some of the other experiments.

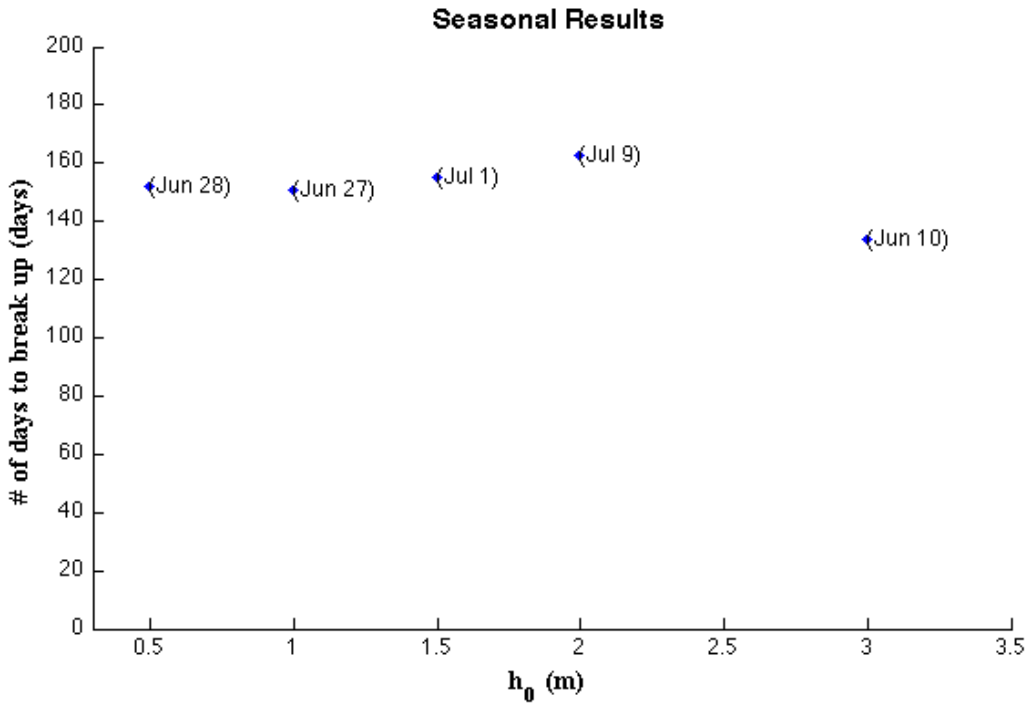

Figure 4.14: Results of the seasonal progressions

Chapter 5

SUMMARY AND CONCLUSION

This study explores how changes in atmospheric and oceanic conditions affect the stability of ice bridges. Following Dumont *et al.* (2009), a sensitivity study was done first to determine suitable conditions for the formation of stable ice bridges. We found that using a cohesion parameter of e=0.9 will allow a stable ice bridge to form at initial thicknesses (h_0) ranging from 0.5m to 3.0m (Figure 3.3).

Once a range of stable ice bridges was determined, atmospheric and oceanic parameters were varied to test their effect on the bridges. The main parameters varied are air temperature, radiative forcing, wind and currents. These parameters were first tested individually. Air temperature, shortwave radiation and long wave radiation were then tested in combinations to determine their combined effects in weakening the stability of the ice bridges. Finally, a seasonal progression was conducted to determine whether the model could simulate bridge disintegration in a timeline similar to nature.

While reviewing the results of the major variable changes, we found bridge formation location to be a key factor on the way ice bridges break. Section 4.1 highlights the three different destruction scenarios found in this study. The "complete collapse" features a full disintegration of the defined ice arch and only occurs for bridges that form at CP1 or recede to that location. The "flowing collapse" occurs for bridges that form at CP2 and features a weakening of the defined ice arch which permits ice to flow into the bottom of the domain. Finally, the "Slow Leak" scenario only occurs for the thickest bridges that form at CP2. Small pieces of ice break off, due to the stress of the incoming ice at the northern

boundary and are deflected to the right due to the Coriolis effect. The defined edge recedes north while the deflected pieces pile on the boundary creating the visual effect of a "leak".

A variety of air temperatures was tested on stable ice bridges of initial thicknesses ranging from $h_0 = 0.5$m to 3.0m. An extreme temperature, for the Arctic, of 30°C introduces enough heat into the system to destroy all ice bridges, regardless of thickness, within under three months. When an air temperature of 20°C is introduced, the bridges take significantly longer to break. The 2.0m bridge takes over 6 months to disintegrate. When the temperature is decreased to a more reasonable Arctic temperature of 10°C, only 0.5m and 0.75m bridges break up in under 8 months. Finally, when the air temperature is 0°C, a more reasonable air temperature for the Arctic, no bridges break in 8 months. Kwok *et al.* (2010) shows that ice bridges in Nares Strait typically last for 5-7 months. Based on this, other parameters must be important for disintegrating ice bridges.

The radiative forcing testing shows that an increase in longwave and shortwave radiation, independently, will not break any ice bridge within 8 months. Thus, radiation increases alone are not strong enough to destroy ice bridges. However, an increase of longwave radiation under an increased air temperature will break the bridges in under 8 months. An air temperature of 30°C introduces too much heat into the system and does not allow for the effects of increased longwave radiation to be seen. However when an air temperature of 20°C is introduced with an increased longwave radiation, the results are more interesting. There is a longwave radiation threshold for strengthening or weakening the ice bridges. Low values of longwave radiation allow ice bridges under 3.0m to persist for a long time. However, 3.0m ice bridges are weakened by the increased amount of incoming ice that is not being melted by the low radiation. This weakening does not occur under higher amounts of longwave radiation. When shortwave radiation is increased in addition to adding 20°C temperature, the shortwave radiation effects prove to be much weaker than the longwave radiation effects. 1.0m and 1.5m bridges do not break under low values of shortwave radiation. 2.0m and 3.0m bridges break the soonest but only due to the incoming ice not being melted by the

shortwave radiation. This happens regardless of how much shortwave radiation is added and highlights the fact that longwave radiation has a stronger effect than shortwave radiation.

When longwave radiation, shortwave radiation and temperature are combined, more reasonable results are obtained for lower, more realistic Arctic air temperatures. Of these three parameters, longwave radiation proved to be the most dominant, followed by air temperature. These results hold for 0.5m and 1.0m ice bridges. 3.0m ice bridges are more effected by ice thickness, particularly the incoming ice, than the other three parameters. The effects of these three atmospheric parameters on the strength of the ice bridge are not as strong as the imposed stress from the 3.0m thick incoming ice. 3.0m bridges typically follow the "slow leak" collapse.

A decrease in wind affects the bridges as expected. The slower the wind, the longer the bridge takes to break. However, this is not seen with the 3.0m bridge. Again, the imposed stress from the 3.0m incoming ice outweighs the effect of the wind on the bridge's strength. Currents, on the other hand, are extremely powerful in ice bridge destruction. 0.50m/s-1m/s currents destroy bridges in only one or two days. Under the exact same thermodynamic conditions, a 0.30m/s current has about the same effect on the 1.0m ice bridge as 10m/s wind.

The study is closed with the testing of a seasonal progression on ice bridges of various thicknesses. All ice bridges break during the seasonal progression, regardless of thickness. The values used in this seasonal progression were averaged from observations. All of the bridges broke up in the model's June or July, which is consistent with the duration of ice bridges in nature. The seasonal progression shows less of a dependance on ice thickness than the other experiments.

One general result found in the temperature analysis, radiation analysis and seasonal progression is the disintegration of the 1.0m bridge before the 0.5m and 0.75m bridges. This is due to the location of the 1.0m ice bridge. The bridge is the weakest and thinnest

bridge to form at the southern constriction point, CP2. In these particular cases, the 1.0m ice bridge is too weak to sustain itself at the southern constriction point in front of the incoming ice from the north. Thus, it was shown to be weaker than the thinner bridges that form at CP1.

The purpose of this study is to explore the effects of atmospheric and oceanic parameter changes on ice bridges. Ice export is a significant factor in the depletion of Arctic sea ice. Nares Strait, despite allowing for significantly less ice export than that through Fram Strait, is a significant passageway (Kwok, 2005). Nares Strait allows for significantly thick, multiyear ice to be exported from the Arctic Ocean, especially when ice bridges do not form (Kwok *et al.* , 2010). Thus, it is important to study how changes in atmospheric and oceanic parameters affect the strength of ice bridges.

Based on averaged observations of temperature and radiation, the seasonal progression shows the ice bridges lasting about as long as they do under our current climate in nature. An increase in temperature, longwave radiation and shortwave radiation, in tandem, will weaken and disintegrate ice bridges much faster. Increases in wind and current speed can also lessen the duration of ice bridges. The longer ice bridges last, the less multiyear ice will be exported out of the Arctic. Thus, it is important to know how a changing climate will affect bridge duration. Our results showed that added shortwave radiation is less effective than longwave radiation due to the reflection from the ice. This reflection effect will be lessened if more ice is exported out of the Arctic due to the shortened duration of ice bridges. Thus, more heat flux will be introduced into the ocean from the shortwave radiation. This added heat flux will weaken the bridges and shorten their duration, completing a positive feedback cycle.

There are improvements to this setup that can be made for future work. The most apparent change could be to strait geometry. This project uses an an idealized strait; a more realistic strait could be used. We've seen in comparing bridge formation to that of Dumont *et al.* (2009), that slight changes in geometry can affect the formation of bridges –

especially the sensitivity to the cohesion parameter e. Using a different cohesion parameter could dramatically affect duration of bridges undergoing added heat flux or dynamic motion.

All parameters in this study are constant over time, with the exception of the seasonal progressions. Having the parameters fluctuate with time would also serve for a more realistic study. The effects of the parameters in this study could be less dramatic if varied over time. For instance, a current speed of 1.0m/s destroyed all of the bridges in this study within 1 day. If the 1m/s current speed was varied over a few hours, perhaps the bridges would last longer.

Bibliography

Brieglab, B.P, & Light, B. 2007. A Delta-Eddington Multiple Scatterting Parameterization for Solar Radiation in the Sea Ice Component of the Community Climate System Model. *NCAR Techincal Note NCAR/TN-472+STR*.

Cheng, W, & Rhines, PB. 2004. Response of the overturning circulation to high-latitude fresh-water perturbations in the North Atlantic. *Climate Dynamics*, **22**(4), 359–372.

Dumont, Dany, Gratton, Yves, & Arbetter, Todd E. 2009. Modeling the Dynamics of the North Water Polynya Ice Bridge. *Journal of Physical Oceanography*, **39**(6), 1448–1461.

Dumont, Dany, Gratton, Yves, & Arbetter, Todd E. 2010. Modeling Wind-Driven Circulation and Landfast Ice-Edge Processes during Polynya Events in Northern Baffin Bay. *Journal of Physical Oceanography*, **40**(6), 1356–1372.

Hibler, W. D. 1979. A Dynamic Thermodynamic Sea Ice Model. *Journal of Physical Oceanography*, **9**.

Hibler, III, W. D., Hutchings, J. K., & Ip, C. F. 2006. Sea-ice arching and multiple flow states of Arctic pack ice. *Annals of Glaciology*, **44**(1), 339–344.

Holland, Marika M., Bailey, David A., Briegleb, Bruce P., Light, Bonnie, & Hunke, Elizabeth. 2012. Improved Sea Ice Shortwave Radiation Physics in CCSM4: The Impact of Melt Ponds and Aerosols on Arctic Sea Ice. *Journal of Climate*, **25**(5), 1413–1430.

Hunke, EC, & Dukowicz, JK. 1997. An elastic-viscous-plastic model for sea ice dynamics. *Journal of Physical Oceanography*, **27**(9), 1849–1867.

Kubat, I., & Sayed, M. 2006. Flow of ice through converging channels. *International Journal of Offshore and Polar Engineering*, **16**(4), 268–273. 16th International Offshore and Polar Engineering Conference (ISOPE 2006), San Francisco, CA, MAY 28-JUN 02, 2006.

Kwok, R. 2005. Variability of Nares Strait ice flux. *Geophysical Research Letters*, **32**(24).

Kwok, R. 2009. Outflow of Arctic Ocean Sea Ice into the Greenland and Barents Seas: 1979-2007. *Journal of Climate*, **22**(9), 2438–2457.

Kwok, R, Cunningham, GF, & Pang, SS. 2004. Fram Strait sea ice outflow. *Journal of Geophysical Research-Oceans*, **109**(C1).

Kwok, R., Pedersen, L. Toudal, Gudmandsen, P., & Pang, S. S. 2010. Large sea ice outflow into the Nares Strait in 2007. *Geophysical Research Letters*, **37**(FEB 9).

Maykut, GA, & McPhee, MG. 1995. Solar heating of the Arctic mixed layer. *Journal of Geophysical Research-Oceans*, **100**(C12), 24691–24703.

Melling, H. 2000. Exchanges of freshwater through the shallow straits of the North American Arctic. *Pages 479–502 of: The Freshwater Budget of the Arctic Ocean*. Springer, New York.

Melling, H. 2002. Sea ice of the northern Canadian Arctic Archipelago. *Journal of Geophysical Research-Oceans*, **107**(C11).

Parkinson, CL, & Cavalieri, D.J. 2008. Arctic sea ice variability and trends, 1979-2006. *Geophysical Research Letters*, **113**.

Stirling, I. 1997. The importance of polynyas, ice edges, and leads to marine mammals and birds. *Journal of Marine Systems*, **10**(1-4), 9–21.

Tremblay, JE, Gratton, Y, Fauchot, J, & Price, NM. 2002. Climatic and oceanic forcing of new, net, and diatom production in the North Water. *Deep-Sea Research Part II-Topical Studies in Oceanography*, **49**(22-23), 4927–4946.

Vihma, Timo. 2014. Effects of Arctic Sea Ice Decline on Weather and Climate: A Review. *Surveys in Geophysics*, 1–40.

Woodgate, RA, & Aagaard, K. 2005. Revising the Bering Strait freshwater flux into the Arctic Ocean. *Geophysical Research Letters*, **32**(2).